TOA Estimation of Unknown Chirp Signal Based on Short Time FRFT and Hough Transform

MengZhu Liu, YiCheng Jiang(✉), Yun Zhang, and Min Jia

Harbin Institute of Technology, Harbin, China
jiangyc@hit.edu.cn

Abstract. This paper studies the time-of-arrival (TOA) estimation problem for unknown chirp signals. The signal envelope is assumed to be trapezoidal, and TOA is defined as the arrival time for envelope to rise to the half-platform value. The current state-of-the-art technique is based on short time fractional Fourier transform (STFRFT). It utilizes STFRFT to obtain the time-profile of time-frequency spectrum, and proves that the profile can be used to estimate TOA. However, this method uses only the peak of profile, which induces information losses and thus degrades the estimation accuracy. To alleviate this, in this paper, Hough Transform is combined with STFRFT to make better use of the time-frequency spectrum. On the other hand, the chirp rate of signal is conventionally assumed to be accurately detected by a previous FRFT step. But the accuracy is actually limited by the computational complexity of FRFT. Hence, a dechirp technique is also involved to make improvements on this aspect. Numerical results show that the dechirp technique brings advantages in detecting chirp rate; and combining Hough Transform with STFRFT is beneficial for TOA estimation.

Keywords: TOA estimation · Chirp signal · FRFT · Hough Transform

1 Introduction

Time-of-arrival (TOA) estimation is an important topic in the area of radar signal processing for its usage in source localization, source identification and signal sorting [1]. In this paper, the TOA estimation of pulse linear frequency modulated (LFM) signal is studied. The signal comes from a noncooperative source so that the parameter is unknown; and the source and sensors are asynchronous. Notably, the estimated TOA can still be used to sort signals or generate the TDOA between different sensors [2].

Two classical TOA estimators are the thresholding estimator (TE) [3] and the auto convolution estimator (ACE) [4]. TE works by comparing signal energy

Supported by National Natural Science Foundation of China 61671490.

M. Jia et al. (Eds.): WiSATS 2019, LNICST 280, pp. 78–87, 2019.
https://doi.org/10.1007/978-3-030-19153-5_8

with a predetermined threshold, and ACE works by taking the auto-convolutions of signals. Some priori information of signal is explored in ACE, which results in its better performance than TE. However, for a chirp signal fractional Fourier transform (FRFT)-type methods can make further improvements since chirp signal is more concentrated in fractional Fourier domain (FRFD)-spectrum than Fourier domain (FD)-spectrum [5,6].

The current state-of-the-art FRFT-type method is short time FRFT estimator (STFRFTE) which is proposed in [7]. For convenience, short time FRFT will be abbreviated as STFRFT. STFRFTE segments the signal by a series of sliding short windows and uses FRFT to obtain the time-profile of STFRFT-spectrum [8]. It is then found that the profile owns a similar shape with signal envelope [7]. On these foundations, the half-peak value of time-profile can be used to estimate TOA.

However, STFRFTE impractically assumes that the signal chirp rate is accurately estimated by a previous FRFT step [7]. The assumption is obviously not reasonable because the accuracy of chirp rate is limited by the searching step of FRFT, which cannot be infinitely small due to complexity limitations. On the other hand, only the peak information of STFRFT-spectrum time-profile is used to determine TOA, which leads to performance losses. Thus, this paper will make improvements on both aspects.

Firstly, by making partial derivatives, it is observed that the precision of an estimated chirp rate is generally inversely proportional to the chirp rate, when the search step is constant. This is because the FRFT-order of signal and the chirp rate thereof are not uniformly one-to-one mapped. Therefore, this paper proposes to iteratively dechirp the signal to reduce its chirp rate, which brings benefits in chirp rate estimation and the subsequent STFRFTE process.

More importantly, Hough Transform (HT) is combined with STFRFTE to generate HT-STFRFTE, where HT is a classic image shape detection technology in automated digital image analysis [9–11]. Since HT makes the information of STFRFT-spectrum more fully used, better results are promised.

The main contributions of this paper are twofold. On one hand, we propose a modified chirp rate estimation technique based on dechirping, which generates DFRFT. Compared with FRFT, it can improve the accuracy of result with the same computational complexity. On the other hand, we propose a novel TOA estimation method based on HT. A HT-based TOA estimation method has been proposed in [12], but its focus is on mapping the signal amplitude into a high-dimension parameter space, which means it is very computationally expensive. Alternatively, we apply HT in FRFT spectrum analysis and the computational cost is very small. We are also aware of some modified HT algorithms, e.g., generalized Hough Transform [13] and randomized Hough Transform [14]. When the signal envelope is not an ideal trapezium, it is an interesting topic for future research to construct modified TOA estimators with them.

Outline of this paper is described as follows. In Sect. 2, the basic signal model is formulated and the STFRFTE method is briefly introduced. Section 3 derives

the DFRFT and HTSTFRFT method. Numerical results are given in Sect. 4 and conclusions are drawn in Sect. 5.

2 Basic Fundamentals

2.1 Signal Model

To start with, the model of pulse LFM signal $x(t)$ is formulated as

$$x(t) = w(t)e^{j\frac{u_0}{2}t^2 + j\Omega_0 t + j\phi_0} \tag{1}$$

where u_0 denotes the chirp rate of $x(t)$, Ω_0 the carrier frequency, ϕ_0 the initial phase and $w(t)$ the signal envelope.

The unknown received signal is

$$s(t) = x(t - \bar{t}_a) + n(t) \tag{2}$$

where $\bar{t}_a$ denotes the time delay between source and receiver and $n(t)$ is the Gaussian white noise.

When source and receiver are synchronous, TOA is $\bar{t}_a$. However, when they are asynchronous, TOA is aliased by a constant C_a, i.e., $t_a = \bar{t}_a + C_a$. Although t_a is an aliased estimate of TOA, it can be estimated by the envelope of received signal ($w(t - t_a)$). Following [7], $w(t - t_a)$ is formulated as

$$w(t - t_a) = \begin{cases} k_r(t - t_a) + \frac{A_0}{2}, & t_1 \le t \le t_2 \\ A_0, & t_2 \le t \le t_3 \\ k_f(t - t_a - t_{PW}) + \frac{A_0}{2}, & t_3 \le t \le t_4 \\ 0, & otherwise \end{cases} \tag{3}$$

where $t_1 = t_a - \frac{t_r}{2}$, $t_2 = t_a + \frac{t_r}{2}$, $t_3 = t_a + t_{PW} - \frac{t_f}{2}$, $t_4 = t_a + t_{PW} + \frac{t_f}{2}$, A_0 is the platform-value of trapezium, t_{PW} the pulse width (PW), k_r the slope of the rising edge, k_f the slope of the falling edge, t_r the duration of the rising edge and t_f the duration of the falling edge. $w(t - t_a)$ is also shown in Fig. 1. As depicted in Fig. 1, the shape of envelope is assumed to be trapezoidal and t_a is defined by the arrival time for $w(t - t_a)$ to rise to $\frac{A_0}{2}$. The purpose of this paper is to estimate t_a through $s(t)$.

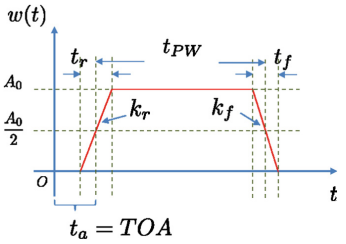

Fig. 1. The ideal envelope of the chirp pulse.

2.2 STFRFT Fundamentals

Since STFRFT is developed based on FRFT, FRFT is firstly described as follows. The pth order FRFT of $x(t)$ is defined as a linear integral transform with kernel $K_p(u,t)$:

$$X_p(t) = F^p[x(t)] = \int_{-\infty}^{\infty} K_p(u,t)x(t)dt \tag{4}$$

where $F^p[\bullet]$ denotes the FRFT operator, $K_p(u,t) = e^{j\pi(t^2\cot\alpha - 2tu\csc\alpha + tu^2\cot\alpha)}$, $\sqrt{1-j\cot\alpha}$, $\alpha = \frac{p\pi}{2}$ (when $p \neq 2n$), $K_{p=4n}(u,t) = \delta(t-u)$ and $K_{p=4n\pm2}(u,t) = \delta(t+u)$. Hence the interval of definition for α is $\alpha \in [-\pi, \pi)$ with period 2π.

According to the principle of FRFT, $|X_p(t)|$ achieves its maximum value when $\alpha = \alpha_0 = \alpha_m + \frac{\pi}{2}$, where $\alpha_m = \arctan(\mu_0)$. Then signal is in the time-frequency line ($\mu_m = \mu_0$) and α_0 is the rotation angle between the time-frequency line and the time domain ($\mu_m = 0$). The geometric relation between $\mu_m = \mu_0$ and α_0 is shown in Fig. 2. For convenience, α_0 is called the matched rotation angle and $p_0 = \frac{2\alpha_0}{\pi}$ is called the matched order, leading to $u_0 = -\cot(\alpha_0)$ and $p_0 = \frac{2}{\pi}\operatorname{arccot}(-u_0)$.

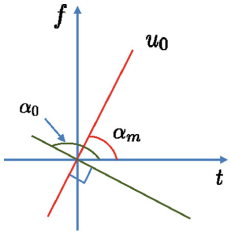

Fig. 2. Geometric relation between the chirp rate u_0 and the matched angel α_0.

STFRFT of $x(t)$ is obtained by multiplying $x(t)$ with a window $g(t)$ before taking the FRFT, that is

$$\underset{x,p}{\mathrm{STFRFT}}(t,u) = \int_{-\infty}^{\infty} x(\tau)g(\tau - t)K_p(\tau,u)d\tau. \tag{5}$$

The performance of STFRFT is affected by the shape and length of the window. Commonly used windows are rectangular window, Gaussian window, etc. As discussed in [15,16], Gaussian window generally leads to the best performance. Thus in this paper, the Gaussian window to be used is expressed as

$$g(t) = (\pi\sigma^2)^{-1/4}e^{-t/2\sigma^2}. \tag{6}$$

where σ is the mean square deviation that determines the length of Gaussian window. According to (5), STFRFT can analyze how the FRFT-spectrum changes by time, which means it is possible to estimate when the signal starts and ends. So an STFRFT-based TOA estimation method (i.e., STFRFTE) was proposed in [7].

2.3 STFRFT-Based TOA Estimation

To perform STFRFT-based TOA estimation, chirp rate μ_0 should be known in prior.

By moving the window, the STFRFT-spectrum at different moments can be obtained. When the window is within the duration of chirp pulse, the peak of STFRFT-spectrum is located at (t, u_0) where t is the window center [6]. Thus along the line $u_0 = -\cot(\alpha_0)$, the time-profile of STFRFT-spectrum $\tilde{w}(t)$ is obtained by

$$\tilde{w}(t) = |\operatorname*{STFRFT}_{x,p_0}(t, u_0)|. \tag{7}$$

In [7], it is proved that TOA is obtainable via

$$\hat{t}_\alpha = \arg\{\tilde{w}(t) = 0.5 \max \tilde{w}(t),\ t < \arg\max_t\ \tilde{w}(t)\} \tag{8}$$

which means, when signal envelope rises to the half of platform-value ($\frac{A_0}{2}$), the STFRFT-spectrum also rises to the half of platform-value in the time-frequency domain in the noise-free situation. This builds the fundamental basis for this paper.

However, STFRFTE has two limitations: (1) Chirp rate is needed in STFRFTE, hence the result is affected by the accuracy of chirp rate estimation; (2) Due to the influences of noise, there is a large fluctuation in the signal amplitude during the pulse duration [16]. To make improvements on these aspects, next section will describe a chirp rate estimation method based on dechirping and a TOA estimation method based on Hough Transform.

3 Proposed Theory and Method

3.1 An Improved Chirp Rate Estimation Method

The chirp rate estimated by FRFT is always erroneous due to the existence of noise and the limitation in computational complexity. Define $\hat{\alpha}_0$ as the estimated matched angle and $\hat{u}_0$ the estimated chirp rate, then $\hat{u}_0 = -\cot(\hat{\alpha}_0)$. It is obvious that the accuracy of $\hat{\alpha}_0$ is determined by the search step length when SNR is high enough. Notably, traditionally the search values of α_0 are uniformly spaced between $\frac{1}{\pi}$ and $\frac{3}{\pi}$, which means the search step is constant.

Hence $\Delta\hat{\alpha}_0$ is almost inevitable and we propose DFRFT to reduce the effect of $\Delta\hat{\alpha}_0$ by exploring the relationship that $\partial\hat{u}_0/\partial\hat{\alpha}_0 = \sin^{-2}\hat{\alpha}_0$, where ∂ denotes the partial derivative notation. Then the derivative is positively correlated with $|\hat{\alpha}_0 - 90°|$, and it reaches the minimum value when $\hat{\alpha}_0 = 90°$. In other words, the smaller $|\hat{\alpha}_0 - 90°|$ is, the more accurate $\hat{u}_0$ is.

On these foundations, we iteratively multiply $s_i(t)$ by $e^{j\hat{u}_i t^2/2}$, where $i = 1, 2, \cdots$, $s_1(t) = s(t)$ and $\hat{u}_i$ is the estimated chirp rate in the ith iteration. In this way, both the chirp rate u_i of $s_i(t)$ and $|\hat{\alpha}_i - 90°|$ can be iteratively reduced which gradually improves the accuracy of $\hat{u}_i$. When the iteration stops, $\hat{u}_0$ is calculated by $\hat{u}_0 = \sum_i \hat{u}_i$.

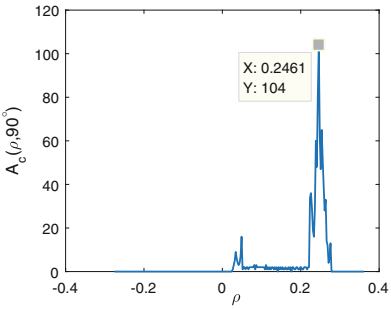

Fig. 3. A typical result of HT.

3.2 STFRFTE Based on Hough Transform

As mentioned before, in STFRFTE, TOA is estimated by finding where the STFRFT-spectrum time-profile $\tilde{w}(t)$ grows to be $\max_t \frac{1}{2}\tilde{w}(t)$. This means TOA should be more accurate with $\max_t \frac{1}{2}\tilde{w}(t)$ approaching the half platform value of $\tilde{w}(t)$. However, $\tilde{w}(t)$ is typically fluctuant with t, leaving $\max_t \frac{1}{2}\tilde{w}(t)$ greatly affected by the local changes of $\tilde{w}(t)$. The value of $\frac{1}{2}\tilde{w}(t)$ is therefore a bad estimator of the half platform-value and a better method is required.

To describe the global feature of the platform-part in $\tilde{w}(t)$, a classical graphics detection theory (i.e., Hough Transform) will be used to identify the graphics components in $\tilde{w}(t)$. It is noteworthy that to combine the graphics detection method with STFRFT is an idea that has not been addressed elsewhere to our best knowledge. The basic theory of Hough Transform is briefly given as follows.

A 2-D straight line (L_1) can be described by the polar coordinate (ρ, θ), where ρ denotes the length of the vertical-line (L_2) from the origin to L_1, θ is the rotation angle of L_2 with the x axis. Then a point (x, y) on L_1 satisfies

$$\rho = x\cos\theta + y\sin\theta. \tag{9}$$

Equation (9) implies that each point on L_1 corresponds to a subset of polar parameter space (e.g., (x, y) corresponds to $(\rho_1, \theta_1), (\rho_2, \theta_2), \cdots$). Then the subsets of different points comprise different curves, which intersect at (ρ, θ). Hence, we define $\boldsymbol{\Theta}_\rho = \{\rho_1, \cdots, \rho_N\}$ as well as $\boldsymbol{\Theta}_\theta = \{\theta_1, \cdots, \theta_N\}$, calculate $\hat{\rho}(\theta_j) = x\cos\theta_j + y\sin\theta_j$ for each θ_j and create a two-dimensional accumulative matrix $\boldsymbol{A_c}$, where the (j_1, j_2)th element of $\boldsymbol{A_c} \in \mathbb{R}^{M\times M}$ is $(\rho_{j_1}, \theta_{j_2})$. Following these, for each θ_j we find ρ_i which belongs to $\boldsymbol{\Theta}_\rho$ while minimizing $||\hat{\rho}(\theta_j) - \rho_i||_2$ and add the (i, j)th element in $\boldsymbol{A_c}$ with 1. Once the points in $\tilde{w}(t)$ are enumerated, the maximum peak of accumulator $\boldsymbol{A_c}$ should generate the required result. Recall that the top line of trapezoid has the value $\theta = 90°$, then the maximum peak $\boldsymbol{A_c}(\rho, 90°)$ is used instead.

Readers are referred to [17] for more implementation details of Hough transform. A typical result of $\boldsymbol{A_c}(\rho, 90°)$ is shown in Fig. 3.

With ρ_e the estimated platform-value (trapezoid height), we have

$$\tilde{w}(t)|_{t=t_a} = 0.5\rho_e,\ t < \arg\max_t \tilde{w}(t). \tag{10}$$

3.3 Implementation Details of DFRFT and STFRFTE

TOA estimation system flow chart is shown in Fig. 4. It should be emphasized that to dechirp signal, TOA is an essential estimate.

Firstly, using FRFT and STFRFTE one can roughly estimate the chirp rate and the TOA of signal. Then the Hough Transform step is used to update the TOA. The estimated chirp rate and TOA can be further used in DFRFT. After iterating several times, one can finally get a high-precision TOA.

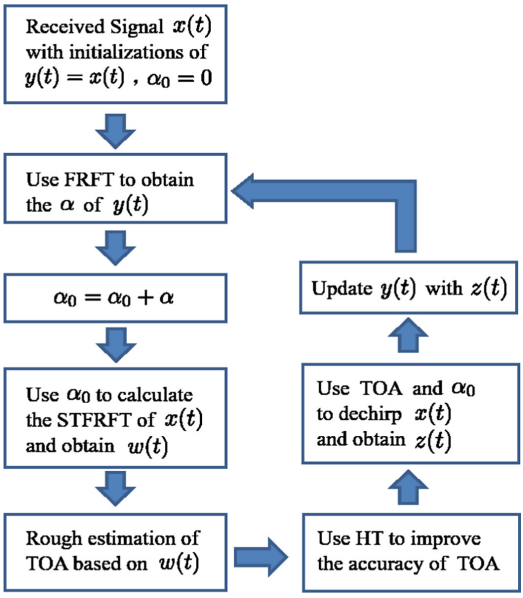

Fig. 4. Flow chart of TOA estimation system.

4 Numerical Results

To illustrate the superiorities of DFRFT and HT-STFRFTE, both FRFT and STFRFTE will be involved for comparison. The parameters of the pulse LFM signal in (1) are $\Omega_0 = 0$, $\phi_0 = 0$, $A_0 = 1$, $t_{PW} = 10\mu s$, $t_r = t_f = t_{PW}/25$ and $k_r = k_f = A_0/t_r$. Sampling frequency is $f_s = 100\,\text{MHz}$ and the chirp rate u_0 is a random variable uniformly distributed between $[\frac{f_s}{2t_{PW}}, \frac{3f_s}{4t_{PW}}]$.

In the simulation for DFRFT, $t_a = 0\mu s$ and there are three times of iteration, with the search steps being $\Delta\alpha_1 = 0.01\pi\,\text{rad}$, $\Delta\alpha_2 = 0.005\pi\,\text{rad}$ and $\Delta\alpha_3 = 0.0025\pi\,\text{rad}$, respectively. In the simulation for HT-STFRFTE, $t_a = 500\,\text{ns}$.

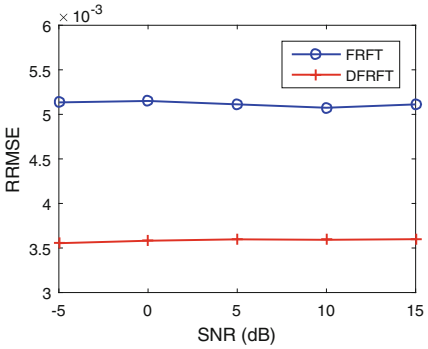

Fig. 5. RRMSEs of the chirp rate estimation in terms of the DFRFT and FRFT.

4.1 Test for DFRFT

In Fig. 5, relative root mean square error (RRMSE) of the estimated chirp rate $\hat{u}_0$ is defined by $\text{RRMSE} = 1/V \cdot \sqrt{\sum_{v=1}^{V} ||\frac{\hat{u}_0 - u_0}{u_0}||_2^2}$, where $V = 200$. RRMSE is used here because it is barely influenced by the value of u_0.

Figure 5 demonstrates the RRMSE curves in terms of DFRFT and FRFT. Since search step can not be infinitely small, the accuracies of DFRFT and FRFT converge to approximately 3.5×10^{-3} and 5×10^{-3}, respectively. We can also observe that DFRFT produces better results than FRFT in the interested SNR range. Thus the novelty of DFRFT is validated.

4.2 Test for HT-STFRFTE

In this subsection, root mean square error (RMSE) of estimated TOA ($\hat{t}_\alpha$) is $\text{RMSE} = 1/V \cdot \sqrt{\sum_{v=1}^{V} ||\hat{t}_\alpha - t_\alpha||_2^2}$, where $V = 200$.

Figure 6 demonstrates the relation between the time-profile of STFRFT-spectrum and its noise-free version. It can be observed that the time-profile of STFRFT-spectrum is fluctuant compared with the noise-free one. The other three curves stand for the estimated half trapezoid height (also the half-platform value). We can see the value estimated by HT-STFRFTE is much closer to the ideal value than that by STFRFTE.

Additionally, Fig. 7 depicts the RMSE curves in terms of HT-STFRFTE and STFRFTE. Clearly, HT-STFRFTE provides better results under both low and high SNR conditions. For example, when SNR = 10 dB, $\text{RMSE}_{\text{STFRFTE}} = 24.2\,\text{ns}$ and $\text{RMSE}_{\text{HT-STFRFTE}} = 16.9\,\text{ns}$. Hence, the benefits from the additional HT step have been certified.

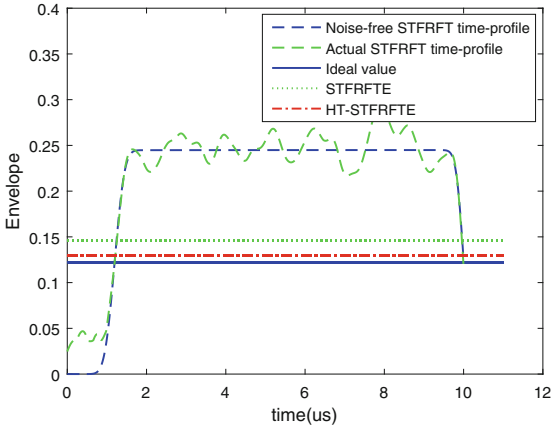

Fig. 6. STFRFT-spectrum time-profile as well as its noise-free version and the estimated half trapezoid heights by HT-STFRFTE and STFRFTE.

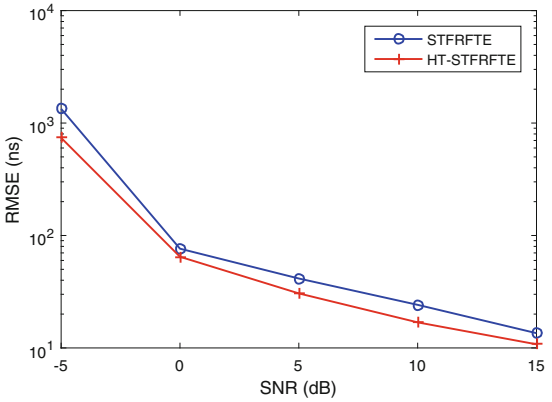

Fig. 7. RMSEs of TOA in terms of HT-STFRFTE and STFRFTE.

5 Conclusion

To estimate TOA of unknown chirp signals, FRFT-type method is studied in this paper. Two contributions are made, i.e., the propositions of dechirp FRFT (DFRFT) and Hough Transform FRFT estimator (HT-STFRFTE), with DFRFT providing the chirp rate required by HT-STFRFTE. DFRFT works by adding an extra step between two iterative FRFT steps, which reduces the signal chirp rate and thus makes the estimated result less sensitive to errors from the search step of matched-order. Compared with FRFT, DFRFT requires approximately the same computational complexity while providing better performances. In STFRFT based TOA estimation, the time-profile of STFRFT-spectrum is observed to fluctuate with the time-frequency domain, which makes the result

sensitive to local changes. Compared with it, HT-STFRFTE can subtract the platform-value more accurately. Numerical results show that, the proposed methods provide better results in terms of chirp rate and TOA.

References

1. Hara, S., Anzai, D., Yabu, T., Lee, K., Derham, T., Zemek, R.: A perturbation analysis on the performance of TOA and TDOA localization in mixed LOS/NLOS environments. IEEE Trans. Commun. **2**(5), 99–110 (2013)
2. Wang, Z.L., Zhang, D.F., Bi, D.Y., Wang, S.Q.: Multiple-parameter radar signal sorting using support vector clustering and similitude entropy index. Circ. Syst. Sig. Process. **33**(6), 1985–1996 (2014)
3. Guvenc, I., Sahinoglu, Z.: Threshold selection for UWB TOA estimation based on kurtosis analysis. IEEE Commun. Lett. **9**(12), 1025–1027 (2005)
4. Chan, Y.T., Lee, B., Inkol, H.R., Chan, F.: Estimation of pulse parameters by convolution. In: Canadian Conference on Electrical and Computer Engineering, CCECE 2006, vol. 2, no. 5, pp. 99–110. IEEE (2016)
5. Almeida, L.B.: The fractional Fourier transform and time-frequency representations. IEEE Trans. Signal Process. **42**(11), 3084–3091 (1994)
6. Ozaktas, H.M., Aytr, O.: Fractional Fourier domains. Sig. Process. **46**(1), 119–124 (1995)
7. Tao, R., Li, Y.-L., Wang, Y.: Short-time fractional Fourier transform and its applications. IEEE Trans. Signal Process. **58**(5), 2568–2580 (2009)
8. Awal, M.A., Ouelha, S., Dong, S.Y., Boashash, B.: A robust high-resolution time-frequency representation based on the local optimization of the short-time fractional Fourier transform. Digit. Sig. Process. **70**, 125–144 (2017)
9. Duda, R.O., Hart, P.E.: Use of the Hough transformation to detect lines and curves in pictures. Commun. ACM **15**, 11–15 (1972)
10. Jiankui, Z., Zishu, H., Sellathurai, M., Hongming, L.: Modified Hough transform for searching radar detection. IEEE Geosci. Remote Sens. Lett. **5**(4), 683–686 (2008)
11. Illingworth, J., Kittler, J.: The adaptive Hough transform. IEEE Trans. Pattern Anal. Mach. Intell. PAMI **9**(5), 690–698 (1987)
12. Sobhani, B.: Target TOA association with the Hough transform in UWB radars. IEEE Trans. Aerosp. Electron. Syst. **52**(2), 743–754 (2016)
13. Ballard, D.: Generalizing the Hough transform to detect arbitrary shapes. Pattern Recognit. **13**, 111–122 (1981)
14. Xu, L., Oja, E., Kultanen, P.: A new curve detection method: randomized Hough transform (RHT). Pattern Recognit. Lett. **11**(5), 331–338 (1990)
15. Durak, L., Arikan, O.: Short-time Fourier transform: two fundamental properties and an optimal implementation. IEEE Trans. Signal Process. **2**(5), 99–110 (2016)
16. Awal, A., Ouelha, S., Dong, S., Boashash, B.: A robust high-resolution time-frequency representation based on the local optimization of the short-time fractional Fourier transform. Digit. Sig. Process. **70**, 125–144 (2017)
17. Mukhopadhyay, P., Chaudhuri, B.: A survey of Hough transform. Priyanka. Pattern Recognit. **48**, 993–1010 (2015)